Auroral poleward boundary intensifications (PBIs): Their two-dimensional structure and associated dynamics in the plasma sheet

E. Zesta,[1] L. Lyons,[1] C.-P. Wang,[1] E. Donovan,[2] H. Frey,[3] and T. Nagai[4]

Received 19 June 2004; revised 21 October 2005; accepted 12 January 2006; published 9 May 2006.

[1] Auroral poleward boundary intensifications (PBIs) are typically seen both in ground meridian scanning photometers (MSP) and in ground and spacecraft auroral images. They appear as a localized increase in intensity at or near the magnetic separatrix. This increase is often seen to extend equatorward through the ionospheric mapping of the plasma sheet. PBIs are associated with plasma sheet flow bursts and are thus important for the remote monitoring of plasma sheet dynamics. From the study of simultaneous ground MSP observations, IMAGE FUV auroral images, and Geotail plasma sheet data, we find that PBIs correlate well with plasma sheet fast flows observed within the local time sector of the PBIs and that there can be several PBIs over the longitudinal range of fast flows in the tail. We infer that every north-south PBI is the ionospheric signature of a fast flow channel in the plasma sheet and that many fast flow channels exist simultaneously over a width of the plasma sheet that can comprise the whole width of the plasma sheet or only a part of it. Also, we find that there is a local time dependence on the type of PBI structure. Most PBIs are narrow auroral structures that are not strictly north-south oriented. Instead, PBIs are tilted counterclockwise away from the north-south direction, leading to a preferred orientation that is approximately aligned with a line going from 0300 magnetic local time (MLT) to 1700 MLT. This results in PBIs that are closer to north-south (NS) structures in the postmidnight sector and closer to east-west (EW) near the dusk sector. In the premidnight sector (2200–0000 MLT), PBIs start as EW arcs and then tilt and become primarily NS structures. We further found for one event that the PBI fast flows have a large V_y component resulting in tail convection that is both earthward and dawnward in the region of Geotail. We suggest that the continuous and strongly positive interplanetary magnetic field (IMF) B_y may order the two-dimensional convection as observed, thus offering a possible explanation for the alignment direction of PBIs in the ionosphere under the assumption that fast flow channels align themselves with the background convection. However, the projection of the PBI structures into the tail using the T96 model suggests that all PBIs, both EW and NS, map to radially stretched channels in the tail that do not have a significant dawnward component. Future work is needed to clarify this apparent contradiction. Finally, frequency analysis indicates that the PBI/bursty bulk flow (BBF) period is characterized by oscillations in the velocity and magnetic field with frequencies of ~0.6 mHz and ~1.3–1.5 mHz. This oscillation in velocity is superposed on the background strong convection.

Citation: Zesta, E., L. Lyons, C.-P. Wang, E. Donovan, H. Frey, and T. Nagai (2006), Auroral poleward boundary intensifications (PBIs): Their two-dimensional structure and associated dynamics in the plasma sheet, *J. Geophys. Res.*, *111*, A05201, doi:10.1029/2004JA010640.

1. Introduction

[2] In order to understand energy, mass and magnetic flux transfer in the magnetosphere, transport in the plasma sheet must be understood. Earthward convection of the tail plasma sheet is an important component of global transport. Up until the early 1990s it was thought that convection in the tail plasma sheet was relatively uniform across the width of the tail. High-speed ion flows were thought to be restricted only in the plasma sheet boundary layer (PSBL) [e.g., *Eastman et al.*, 1984, 1985]. *Baumjohann et al.* [1990]

[1]Department of Atmospheric and Oceanic Sciences, University of California, Los Angeles, California, USA.
[2]Physics Department, University of Calgary, Calgary, Alberta, Canada.
[3]Space Sciences Laboratory, University of California, Berkeley, California, USA.
[4]Department of Earth and Planetary Sciences, Tokyo Institute of Technology, Tokyo, Japan.

0148-0227/06/2004JA010640

were the first to show that high-speed flows occur all through the plasma sheet and not only in the PSBL. Baumjohann et al. used Active Magnetospheric Particle Trace Explorers Ion Release Module (AMPTE/IRM) data (spacecraft orbit -9 to -19 R_E) to show that for high *AE* index it is more probable to detect fast flows in the central current sheet (CS) than in the PSBL. *Angelopoulos et al.* [1992, 1994] used data from AMPTE/IRM and ISEE2 and did a wide and comprehensive statistical study of fast flows in the plasma sheet. *Angelopoulos et al.* [1992, 1994] found that fast flows organize themselves in 10-min flow intervals, which were named bursty bulk flows (BBFs). Note that in the remainder of this paper we will use the terms "BBF" and "tail fast flow" interchangeably. Inside the BBF interval the flow exhibits peaks at ~1-min intervals. The most important conclusions of the *Angelopoulos et al.* [1992, 1994] studies are (1) plasma sheet flows can be bursty during both geomagnetically quiet and disturbed times in the central plasma sheet and (2) BBFs can be responsible for 60–100% of the measured earthward transport of mass, energy, and magnetic flux in the spatial domain covered by the satellite measurements, even though the BBFs occurred during only 10–15% of the observation time.

[3] Once the importance of the central plasma sheet fast flows (BBFs) for the transport was established, the natural consequence was to search for the ionospheric signature of the BBFs. In situ observations of BBFs are sparse and can only offer information on a single point within the plasma sheet region. The nightside ionosphere on the other hand is a mirror of the whole tail plasma sheet. If the ionospheric signature of BBFs is accurately identified, then the ionosphere can be used to remotely study the dynamics of plasma sheet transport via fast flows from sequences of ionospheric images.

[4] *Henderson et al.* [1998] and *Sergeev et al.* [1999] showed, albeit indirectly, that north-south aligned auroral forms that often appear on the nightside during disturbed conditions (also called "streamers") may be a signature of rapid, transient flows in the central plasma sheet (CPS). *Lyons et al.* [1999] used data from ground-based meridian scanning photometers (MSP) and the Geotail spacecraft to show that periods of repetitive, transient, tail flow bursts are associated with periods of auroral poleward boundary intensifications (PBIs). PBIs are intense, transient auroral disturbances that initiate at the separatrix and then typically move equatorward [*Lyons et al.*, 1999; *Zesta et al.*, 2002]. *Lyons et al.* [1999] were only able to do a general correlation between PBIs and tail fast flows (BBFs), but *Zesta et al.* [2000] did, for the first time, a one-to-one correlation between five distinct PBIs with five equally distinct BBFs in the tail. *Zesta et al.* [2000] were also able to show that the five PBIs were north-south auroral structures that moved equatorward and westward. *Sergeev et al.* [2000] were also able to directly associate an auroral streamer with a BBF in the tail. *Kauristie et al.* [2000, 2003] studied the ionospheric current structure and optical signatures of auroral streamers and showed that their characteristics are consistent with fast flow channels. *Nakamura et al.* [2001b] further studied the association between tail fast flows and auroral streamers or activations. Perhaps the most important result from the *Nakamura et al.* [2001b] study is that tail fast flows that are associated with streamers occur tailward of 16 R_E, while fast flows associated with activations and expansions (like pseudobreakups) occur earthward of 16 R_E. This study further established the fast flows associated with PBIs as a midtail phenomenon.

[5] *Zesta et al.* [2002] conducted a detailed study on the two-dimensional structure of PBIs, which cannot be determined solely from MSP observations. Zesta et al. found that PBIs, as observed by the MSPs, are either equatorward extending or nonequatorward extending. Equatorward extending PBIs are either north-south aligned structures or east-west arcs propagating mostly equatorward, but *Zesta et al.* [2002] were not able to determine without doubt which type is the most prevalent. They suggested that equatorward extending PBIs may be the auroral footprint of two major modes of energy transfer in the plasma sheet: multiple, narrow, earthward fast flow channels and sequences of azimuthally broad and primarily earthward propagating phase fronts initiating near the separatrix. Nonequatorward extending PBIs were found to mostly be a series of multiple bead-like intensifications along the poleward boundary of the aurora zone without an equatorward extending feature. Such PBIs may be evidence for shear instabilities at the separatrix boundary on the flanks of the magnetotail.

[6] The *Zesta et al.* [2002] results combined with the results of studies that associate auroral forms with BBFs [e.g., *Zesta et al.*, 2000; *Sergeev et al.*, 2000, *Nakamura et al.*, 2001a] suggest that at least some equatorward extending PBIs are associated with BBFs in the tail. The question is whether all equatorward extending PBIs, be they north-south or east-west structures, are associated with BBFs and if there are any differences between these two auroral forms.

[7] In the present study, we use ground MSP data to identify PBIs during an active period, auroral images from the IMAGE spacecraft to identify the true shape of the PBIs and how they fit into the global nightside auroral activity, and in situ Geotail data from the midtail to identify fast flows. We study in detail the period 0200–0800 UT on 3 January 2001, a relatively active period and when all three data sets were available in good conjunction.

2. Observations

[8] The ground MSP observations are from the CANOPUS station at Rankin Inlet. IMAGE auroral observations are from the FUV imager [*Mende et al.*, 2000], which has good spatial resolution and the added benefit of spending a significant amount of time (several hours) with the full nightside aurora in its field of view. That gives us the opportunity to view PBIs in a global perspective and to see how they fit with the background aurora and develop over several hours. We also use in situ Geotail magnetic field data from the fluxgate magnetometer [*Kokubun et al.*, 1994] and plasma data from the low-energy particle (LEP) instrument [*Mukai et al.*, 1994] from within the tail plasma sheet. Finally, solar wind and interplanetary magnetic field (IMF) observations are from the ACE Solar Wind Electron Proton Alpha Monitor (SWEPAM) [*McComas et al.*, 1998] and from the Magnetic Fields Instrument (MAG) [*Smith et al.*, 1998], respectively.

2.1. Ground and Plasma Sheet Observations

[9] Figure 1 is a general overview of the studied event, 3 January 2001. Ground auroral and solar wind observations

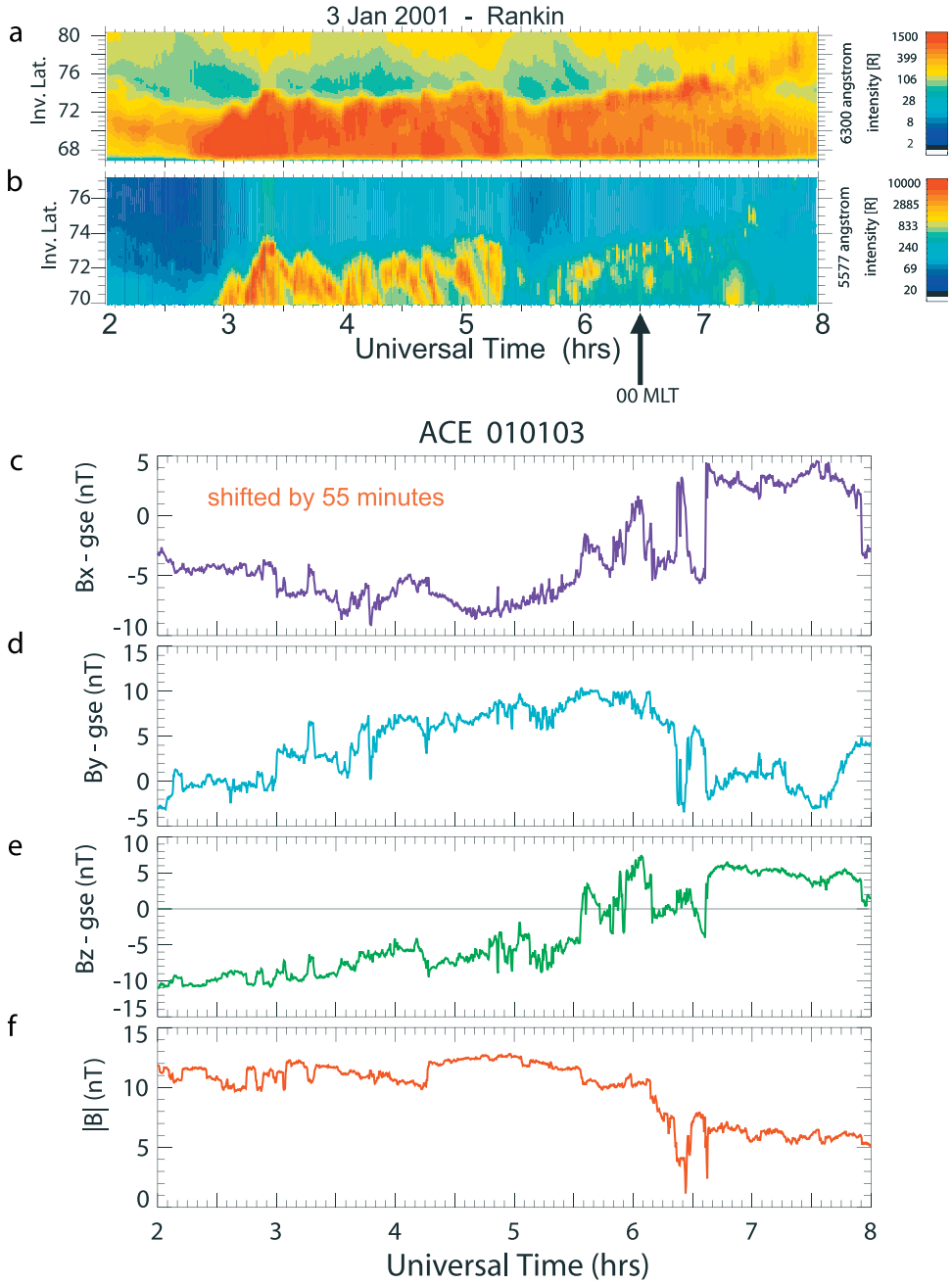

Figure 1. General overview of the studied event, 3 January 2001: Ground auroral and solar wind observations for the 0200–0800 UT period. (a, b) Emissions from the Rankin Inlet meridian scanning photometer (MSP); (c, d, e, f) Interplanetary magnetic field (IMF) data from the ACE spacecraft.

are shown for the 0200–0800 UT period. Figures 1a and 1b show emissions from the Rankin Inlet meridian scanning photometer (MSP) and Figures 1c, 1d, 1e, and 1f show IMF data from the ACE spacecraft located in orbit around the L1 point between the Sun and the Earth. Emissions from the Rankin MSP are shown in the 6300 Å and 5577 Å wavelengths versus invariant latitude and time. The MSP completes one full meridional scan every minute and, by assuming that all emissions for a particular wavelength come from a set altitude (230 km for the 6300 Å and 110 km for the 5577 Å emissions), we convert the measured emission intensity versus zenith angle to intensity versus invariant latitude. 6300 Å emissions are a manifestation of soft electron precipitation and diffuse aurora while 5577 Å emissions are a manifestation of harder electron precipitation and discrete aurora. PBIs typically appear in the 5577 Å emissions and are thus associated with discrete aurora. The poleward boundary of the 6300 Å emissions lies within ~1°–2° of the separatrix boundary [*Blanchard et al.*, 1997], and in Figure 1 this boundary traces the poleward edge of the red/orange-colored emissions. The magnetic meridian of Rankin passes through magnetic local midnight at 0630 UT, denoted in Figure 1 with an arrow. Magnetic field data from ACE are shifted by 55 minutes to account for solar

wind advection from the location of ACE to the Earth's magnetosphere.

[10] The IMF is strongly southward until ~0530 UT, when it turns northward, oscillates around 0 nT for 1 hour and then remains steady northward for a few hours. IMF B_y is strongly positive until ~0630 UT. These IMF conditions and their changes are reflected in the MSP emissions. There is a substorm onset at ~0230 UT (the onset is not seen in the Rankin emissions as it occurred at a latitude lower than the field of view of the MSP, but was seen in ground magnetometers) with two or three intensifications, and the recovery phase begins at ~0325 UT. Activity remains high after that as the magnetosphere continues to be strongly driven by the very negative IMF B_z, and we observe a series of equatorward extending PBIs up until 0530 UT. At 0530 UT, simultaneously with the northward turning of the IMF, the emission intensity decreases significantly and the auroral poleward boundary drifts slowly poleward (as evidenced by the poleward boundary of the 6300 Å emissions). The time period studied in the present paper is the period following the substorm from 0320 UT to 0530 UT, while IMF B_z was strongly negative and IMF B_y was strongly positive.

[11] Figure 2 shows plasma and magnetic field parameters measured in the tail by Geotail during the time period 0200–0800 UT. At that time, Geotail was in the midtail at $X_{GSM} \cong -21\ R_E$ and was moving away from the noon-midnight meridian toward dawn. Plotted from top to bottom are the x, y, and z GSM components of the magnetic field (Figures 2a, 2b, and 2c), the magnitude of the magnetic field (Figure 2d), the x, y, and z components of the ion velocity (Figures 2e, 2f, and 2g), the ion density (Figure 2h), temperature (Figure 2i), and the ion pressure (Figure 2j, thin line) and total pressure (Figure 2j, thick line). The dashed lines in Figures 2a–2d are the T96 model magnetic field at the location of Geotail, which will be discussed later. In Figure 2e, along with V_x (light line), we plot $\mathbf{V}_{\perp \mathbf{x}}$ (heavy line), that is, the component of the perpendicular-to-**B** velocity along the X_{GSM} line. We expect fast flows in the plasma sheet to be primarily in the x direction. These are mostly parallel to **B** in the plasma sheet boundary layer (PSBL) and perpendicular to **B** closer to the central current sheet. Most BBFs from ~0410 to 0540 UT have their x component flow primarily perpendicular to **B**. This is as expected, since the plasma and total pressure are nearly equal during this period, and B_x is structured and relatively small, implying that Geotail was near the center of the plasma sheet during this period. Focusing on Figures 2a and 2j we conclude that Geotail is inside the plasma sheet throughout the time period plotted, 0200–0800 UT. From 0200 to 0220 UT Geotail is close to the current sheet, while during much of the period from 0200 to 0400 UT the magnetic pressure dominates ion pressure and B_x is large so that the spacecraft is closer to the plasma sheet boundary layer. After 0540 UT Geotail is continuously within the plasma sheet, but somewhat away form the center of the current sheet and from the plasma sheet boundary layer.

[12] There are no fast flows (at least not with speed >200 km/s) before 0400 UT. We do see however a dipolarization at 0240 UT, associated with the substorm onset near that time. Repetitive BBFs occur between 0400 and 0540 UT. The first BBF after 0400 UT is mostly parallel to **B** and is associated with a brief excursion of the spacecraft near the PSBL. After that, BBFs are mostly perpendicular to **B** and are observed close to the central current sheet. After 0540 UT there are no significant fast flows until an isolated one at ~0650 UT, which we will not examine here because we have no IMAGE FUV data from that time.

[13] Figure 3 combines the MSP 5577 Å emissions with the key Geotail observations from Figures 1 and 2 for the period 0230–0600 UT. Plotted from top to bottom are the 5577 Å emissions (Figure 3a), the V_x plasma velocity and the x component of the perpendicular-to-**B** velocity $\mathbf{V}_{\perp \mathbf{x}}$ (Figure 3b), the V_y velocity (Figure 3c), the plasma β parameter (Figure 3d), and the total pressure and ion pressure (Figure 3e). The plotted β parameter in Figure 3 is a more sensitive measure of whether the spacecraft is located in the central plasma sheet or in the lobes [e.g., *Baumjohann et al.*, 1988; *Sergeev et al.*, 2000] than just looking at the ion and total pressures, as we did in discussing Figure 2. For small β ($\beta < 1$), as in the 0230–0245 UT and 0345–0415 UT periods, we consider that Geotail is in the PSBL and very close to the lobes. For very large β, Geotail is in the central plasma sheet. It is now easier to see that after about 0415 UT, while the large BBFs flowing perpendicular to **B** are occurring, Geotail is often in the central current sheet.

[14] We will focus our attention on the PBIs and fast flows that occurred between 0320 and 0545 UT. There are repetitive and continuous equatorward extending PBIs in the MSP data during this period. The PBIs begin immediately after the end of the substorm expansion phase, at 0320 UT, and before fast flows are observed at Geotail, after 0400 UT. Also fast flows continue until ~0545 UT, which is longer than the PBIs observed at Rankin Inlet, which end at ~0520 UT. There is thus only a general association between PBIs and BBFs rather than the one-to-one association found by *Zesta et al.* [2000]. This is because, as discussed in section 2.2, Rankin Inlet is in the premidnight region during this period whereas Geotail is in the dawn sector of the plasma sheet. The earthward x velocity during the BBFs reaches values as high as 600 km/s. However, during the 0400–0600 UT period the ion velocity is not always earthward; the bursts of fast earthward flow alternate with smaller burst of tailward flow of up to −200 km/s. Thin horizontal lines in Figure 3 indicate the zero level in both V_x (Figure 3b) and V_y (Figure 3c). Thus it seems that for this 3-hour period the velocity along the x direction oscillates between earthward and tailward with the earthward velocities being much larger in magnitude. Furthermore, during that same time period the y component velocity bursts are primarily dawnward (i.e., negative). These V_y bursts are as large as −300 km/s, and they also alternate with smaller bursts of duskward (positive) V_y velocity. This means that the average plasma sheet flow is earthward and dawnward, but this flow occurs in bursts that alternate with flow in different directions. We will discuss this interesting observational feature later in section 3.

[15] Each fast earthward flow burst in Figure 3 is accompanied by a pressure and temperature reduction, by increases in the total magnetic field, and by peaks in dawnward directed V_y. Vertical dashed lines in Figure 3 indicate the onsets of most BBFs and the changes in their plasma and magnetic field properties (for changes in the

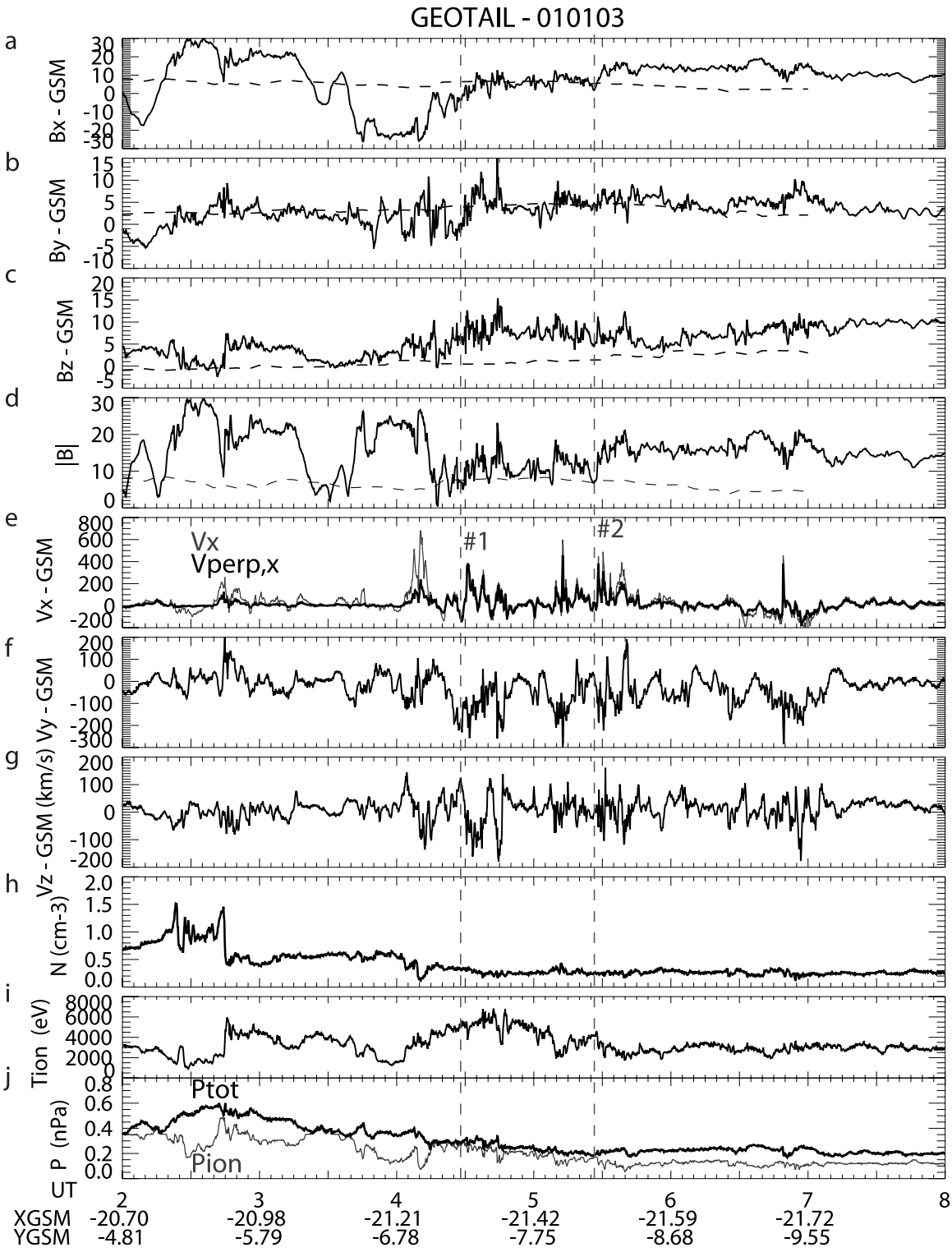

Figure 2. Plasma and magnetic field parameters measured in the tail by Geotail during the time period 0200–0800 UT. (a, b, c) *x*, *y*, and *z* GSM components of the magnetic field; (d) magnetic field magnitude; (e, f, g) *x*, *y*, and *z* components of the ion velocity; (h) ion density; (i) temperature; and (j) ion pressure (thin line) and total pressure (thick line). Dashed lines in Figures 2a–2d are the T96 model magnetic field at the location of Geotail.

temperature look at the two examples in Figure 2 indicated by the two vertical dashed lines). Note that the small increases in the B_z component of the magnetic field during the BBFs (see two examples in Figure 2) are not dipolarizations as both the B_x and B_y components of the magnetic field increase during the BBF. The most widely accepted mechanism for the generation of BBFs in the tail is the plasma "bubbles" model [*Chen and Wolf*, 1993]. These are

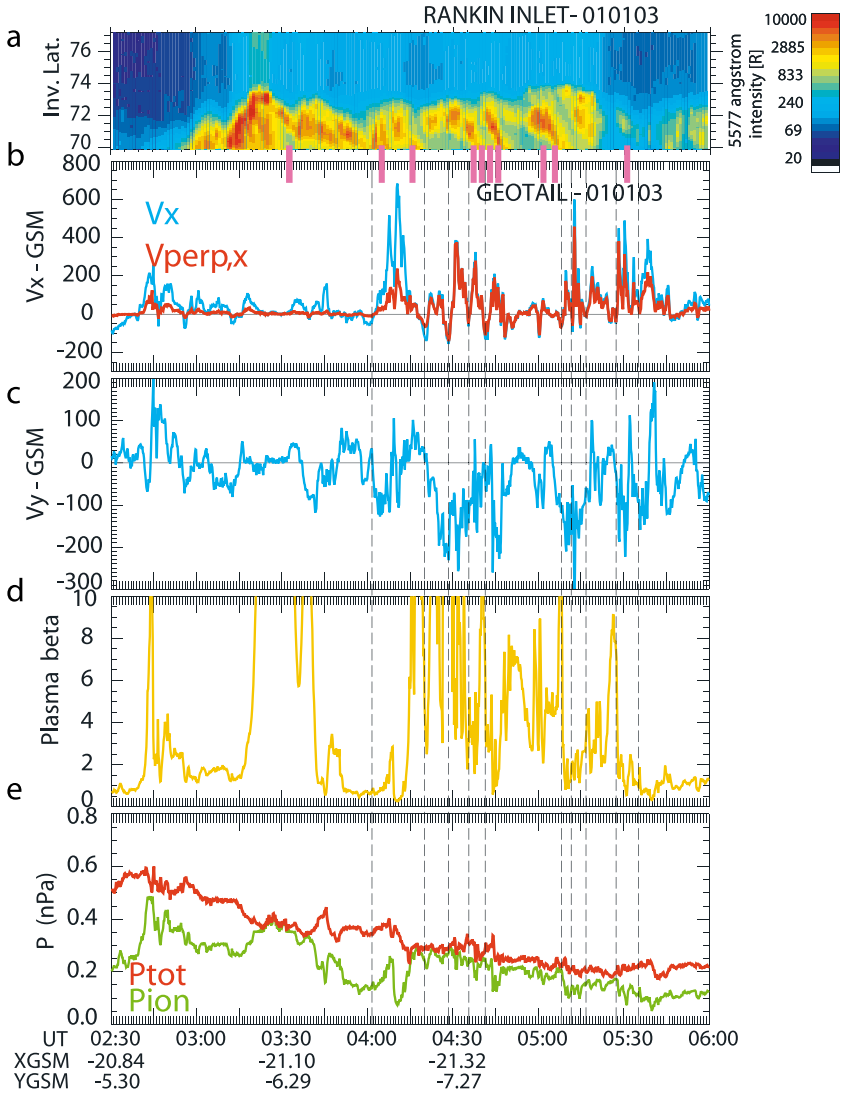

Figure 3. MSP 5577 Å emissions and the key Geotail observations for the period 0230–0600 UT. (a) 5577 Å emissions; (b) V_x plasma velocity and x component of perpendicular-to-**B** velocity $\mathbf{V}_{\perp \mathbf{x}}$; (c) V_y velocity; (d) plasma β parameter; and (e) total pressure and ion pressure. Ten vertical purple bars between Figures 3a and 3b indicate times for which global auroral images from the IMAGE FUV instrument in Figure 4a are shown.

localized, underpopulated flux tubes originating in the distant tail that move earthward at high speeds because of a polarization electric field within the bubble. The main characteristics of a bubble are low density and pressure with respect to the ambient environment and high magnetic field. All of the BBFs in Figure 3 satisfy these criteria.

2.2. IMAGE Observations

[16] Figure 4a shows data from the IMAGE spacecraft FUV auroral imager [*Mende et al.*, 2000]. It includes a series of 10 representative images from the time period shown in Figure 3. The times of the selected images are indicated in Figure 3 by the short vertical purple bars between Figures 3a and 3b. In every image in Figure 4a only the nightside portion of the aurora is shown and the lines of 1800, 2100, 0000, 0300, and 0600 MLT are plotted. The red circle in each image of Figure 4a indicates the field of view at Rankin Inlet for 5577 Å emissions, based on a 170° field of view projected to 110 km altitude. The dot in the middle of each circle is the location of Rankin, and the MSP measures only on a line along the north-south meridian. Notice that during the event, Rankin Inlet moved from 2100 MLT to 2300 MLT. The red diamond in the postmidnight sector of each image shows the ionospheric footprint of Geotail mapped using the T96 model [*Tsyganenko*, 1996], which remains in the 0130–0230 MLT region. We discuss the images in Figure 4a in time sequence (from left to right and then from top to bottom) and refer to the relevant data of Figure 3.

[17] 1. Before ~0405 UT (Figure 4a (top) and first two bars in Figure 3), there is no aurora in the local time sector of the Geotail ionospheric footprint, and no significant fast flows are seen in Figure 3. This implies that when no PBIs are observed within a local time sector in the aurora no fast flows are occurring in the tail within the same local time sector. At the local time of Rankin, the global auroral

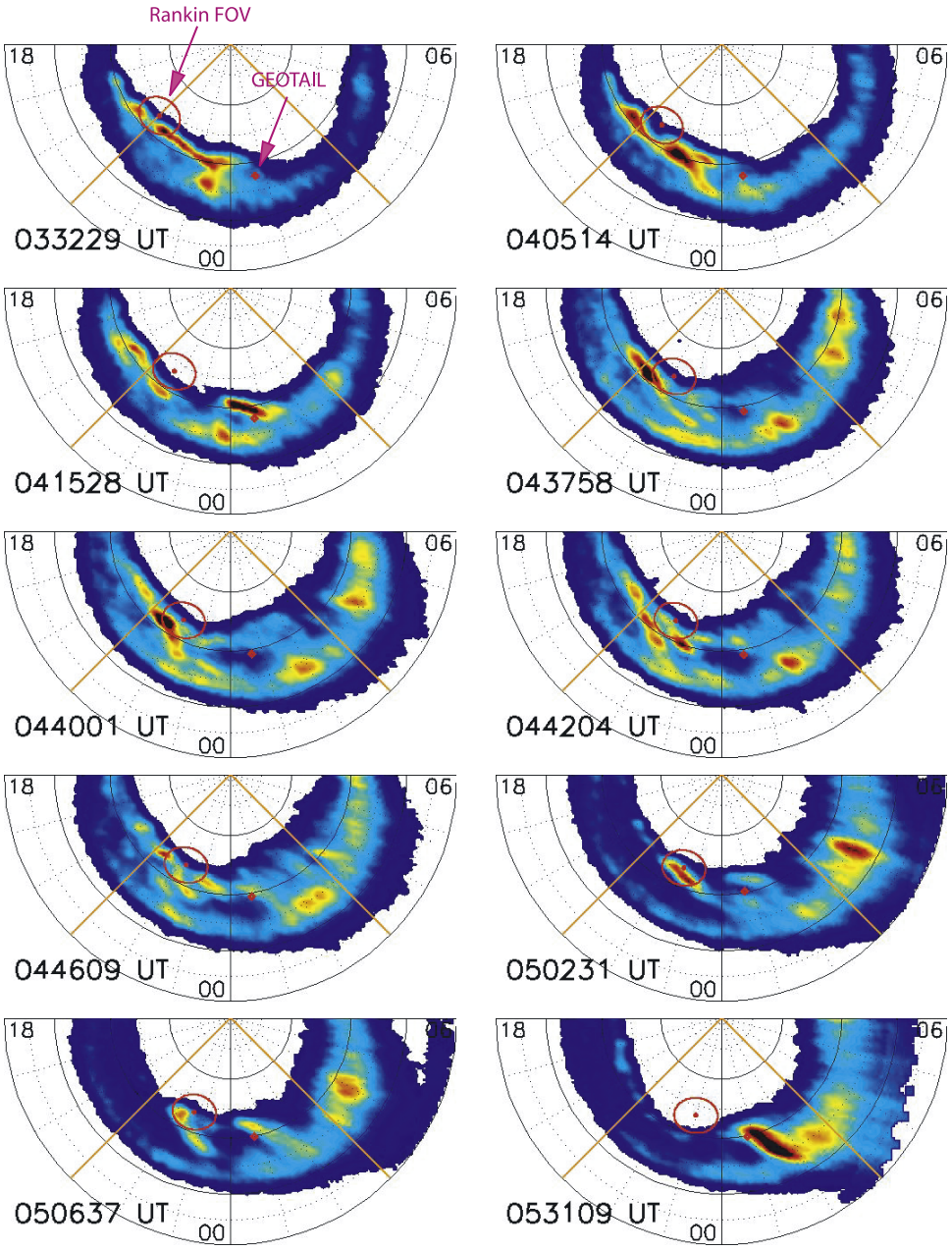

Figure 4a. Data from the IMAGE spacecraft FUV auroral imager: 10 representative images from the time period shown in Figure 3.

images show that the PBIs observed by the ground MSP during this period are primarily east-west arcs as seen in the global auroral images. This is seen in much better spatial detail in Figure 4b, which shows a DMSP optical image from the Operational Linescan System (OLS) instrument (data online at the National Geophysical Data Center) of the aurora that is available for the same time as the FUV image of 0355:00 UT. The DMSP image (Figure 4b) shows multiple east-west arcs. The location of Rankin in the DMSP image is indicated by the red solid star.

[18] 2. At 0415:28 UT (Figure 4a, third image and third bar in Figure 3), auroral activity has now moved over the local time sector of the Geotail footprint. A primarily NS PBI is seen over Geotail's footprint, and now strong flows are observed at Geotail (Figure 3). Rankin is observing different PBIs, still primarily EW arcs. The previous two images showed no postmidnight PBI activity and Geotail showed no BBFs in the same local time sector. Now we see that when PBIs are observed at a local sector in the aurora, fast flows are seen in the tail in that same local sector as well. This shows that one-to-one correlations between PBIs and plasma sheet fast flows should only be observed when there is a good local time conjunction between the observed PBIs and observations within the plasma sheet.

[19] 3. At 0437:58 UT to 0446:09 UT (Figure 4a, fourth through seventh images and fourth through seventh bars in Figure 3) the next four images are from a period of ~15 minutes, when the ground MSP is observing two clear equatorward extending PBIs in the premidnight sector while Geotail observes a series of fast flows in the postmidnight

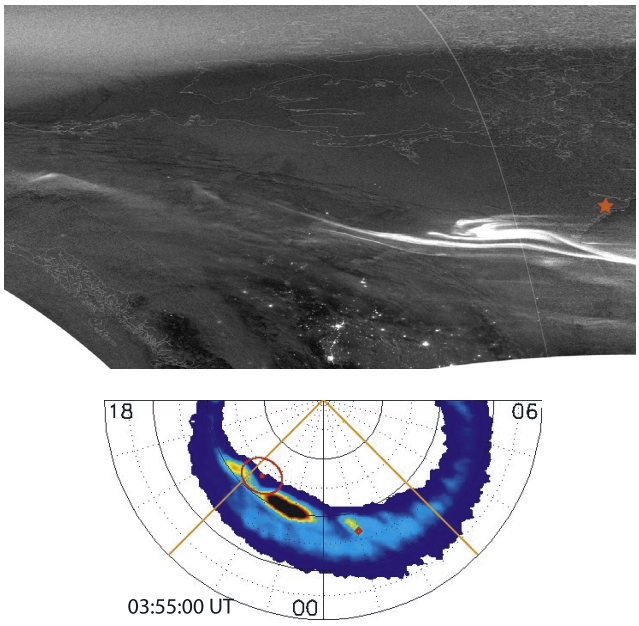

Figure 4b. (top) DMSP optical image from Operational Linescan System (OLS) instrument of the aurora that is available for the same time as (bottom) FUV image of 0355:99 UT.

sector. Geotail also observes large V_y velocities and large β (the spacecraft is in the central current sheet). From the FUV images we see that PBIs are observed at both the Geotail ionospheric footprint and the Rankin locations. The PBIs in the premidnight region start from EW arcs that turn to become primarily NS structures. NS PBIs continue to be observed in Geotail's local sector. It is interesting to note that, only on the basis of Figure 3, it might be tempting to assign a direct correlation between the PBIs observed at Rankin and the fast flows observed at Geotail. The global perspective given by the FUV images corrects this erroneous perception. The image of 0446:09 UT is particularly illuminating in that respect. It shows clearly that many PBIs are occurring at the same time across the width of the nightside oval, over MLTs 1800–0400. All PBIs are similar and they seem to be aligned along a line that goes through the 1700 and 0300 MLTs. PBIs closer to the dusk sector are thus seen as mostly east-west arcs. PBIs in the premidnight region start as east-west arcs along the poleward boundary of the aurora; subsequently they tilt and become primarily NS structures (most clearly observed in the images of 0442:04 UT and 0446:09 UT). PBIs in the postmidnight region are primarily NS structures aligned approximately along the 1700–0300 MLT line.

[20] 4. At 0502:31 UT to 0506:37 UT (Figure 4a, eighth and ninth images and eighth and ninth bars in Figure 3), the MSP at Rankin observes a clear equatorward extending PBI in Figure 3. From the images we see that this starts as an EW arc, which quickly rotates to a primarily NS structure. At the same time the ionospheric footprint of Geotail is located in a similar but different NS structure associated with the BBFs observed at the time.

[21] 5. By 0531:09 UT (Figure 4a, tenth image and tenth bar in Figure 3) no aurora and no PBIs are seen over the field of view of Rankin in agreement with the MSP observations of Figure 3. From Figure 3 it is seen that even though PBIs are no longer observed by the MSP at Rankin, fast flows continue to be observed by Geotail. Also, IMAGE FUV shows that even though there are no PBIs over Rankin, there is a distinct NS PBI over Geotail's footprint in the postmidnight region, which would then be associated with the fast flows observed within the plasma sheet.

3. Analysis of the Observations

[22] Global observations of the nightside auroral oval from the IMAGE FUV imager in conjunction with the ground MSP and the in situ Geotail observations showed that (1) there are many PBIs across the width of the oval and each PBI is associated with a fast flow channel occurring in the same local time sector as the PBI, (2) PBIs are mostly east-west (EW) arcs when they occur near the dusk sector, EW arcs that turn to NS structures at premidnight, and NS structures at postmidnight, and (3) bursts of earthward fast flow alternate with smaller bursts of tailward flow. We further investigate these observational results in this section.

3.1. Frequency Analysis of Tail Properties

[23] We have already seen, in the discussion of Figure 3, that the ion velocity observed by Geotail is not strictly earthward; intervals of earthward flow alternate with intervals of tailward flow. We can see this more clearly in Figure 5 where we plotted the total velocity vector in the XY plane approximately every 24 s along the path of the Geotail spacecraft for the 0400–0600 UT period, when the repetitive BBFs are occurring. Vectors that have a positive (i.e., earthward) V_x are plotted in red and the ones with tailward V_x are plotted in blue. Two things become immediately apparent while inspecting Figure 5. First, the vectors do not simply flip from earthward to tailward, rather they harmonically rotate from earthward to tailward and back; and second, the vectors obtain their largest magnitude when pointing earthward and dawnward (not strictly earthward) and at a significant angle from the x direction.

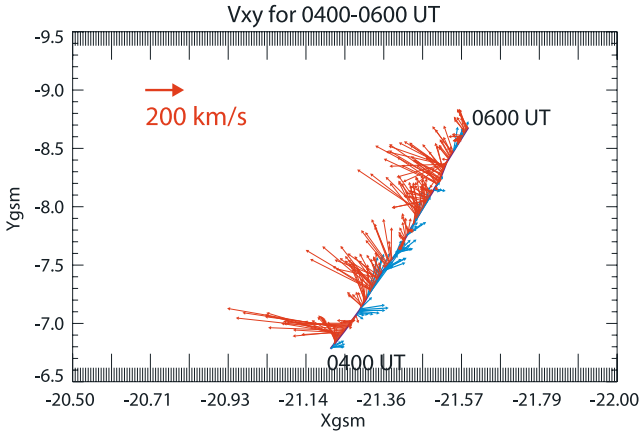

Figure 5. Total velocity vector in the XY plane plotted approximately every 24 s along path of the Geotail spacecraft for the 0400–0600 UT period, when repetitive bursty bulk flows were occurring. (red) Vectors that have a positive (i.e., earthward) V_x. (blue) Vectors that have tailward V_x.

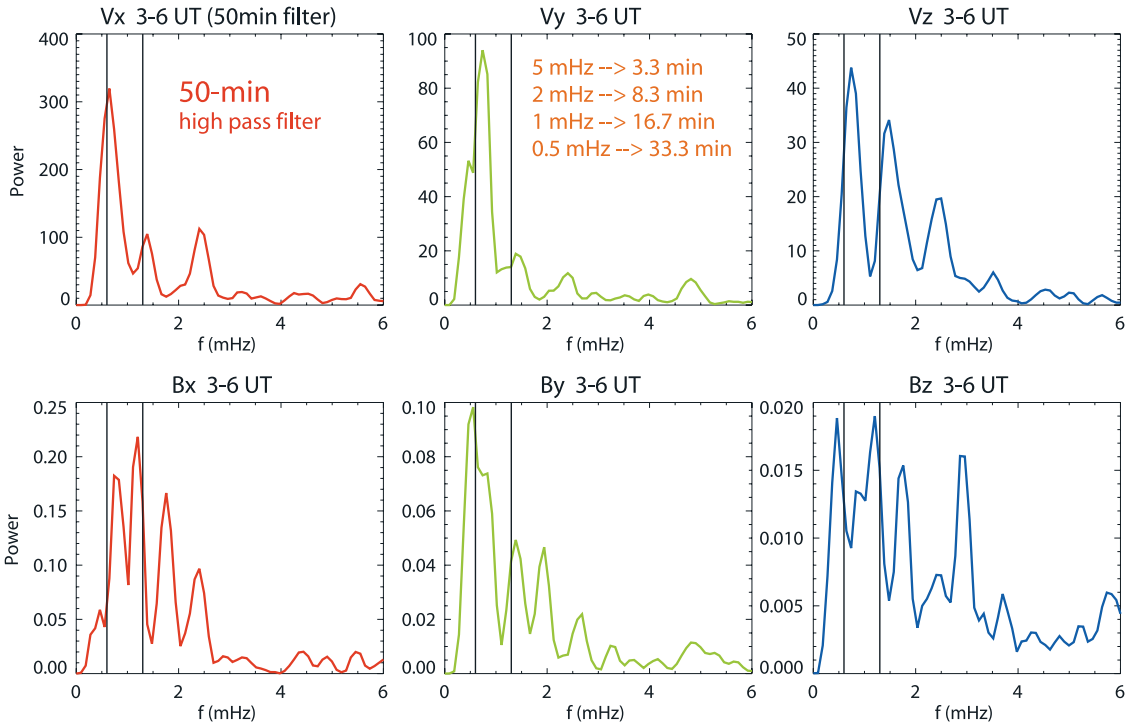

Figure 6. Power spectra for the three components of the (top) ion velocity and (bottom) magnetic field. Two vertical lines in each portion of Figure 6 indicate frequencies of 0.6 mHz and 1.3 mHz.

[24] We will discuss the first observation from Figure 5, that is, the oscillation of the V_{xy} vector between earthward and tailward. The period of this oscillation is ~15 minutes and the earthward bursts of the cycle seem to last longer and have larger amplitudes. There is some prior evidence supported by theoretical studies that ULF waves in the form of waveguide modes may exist in the magnetotail [e.g., *Allan and Wright*, 2000; *Mann et al.*, 1999]. Such waves could be excited by flows in the magnetosheath [*Mann et al.*, 1999] and they should be observed in situ in the tail in both the magnetic field and plasma properties. More recently, *Lyons et al.* [2002] showed evidence that significant ULF power in the 0.5–0.7 mHz frequency (25–30-min period) and its first harmonic at 1.1–1.3 mHz exists simultaneously in the plasma sheet, in the inner magnetosphere (magnetic field and energetic particle fluxes), in the intensities of auroral PBIs, and in ground magnetic field data. These observations indicate the existence of a global large-scale ULF oscillation in the Earth's magnetotail. *Lyons et al.* [2002] were not able to identify if such a global oscillation is externally driven or internally triggered. *Kepko and Spence* [2003] have recently shown evidence that global magnetospheric ULF oscillations for six events may have been directly driven by solar wind density variations [see also *Samson and Rankin*, 1994].

[25] Figure 5 indicates that the ion flow in the plasma sheet does have an oscillation frequency in the ULF range. Figure 6 shows power spectra for the three components of the ion velocity (top) and magnetic field (bottom). We first applied a high-pass filter in the time series data with a cutoff frequency of 0.33 mHz (period of 50 min, i.e., the filter cuts off all periods longer than 50 minutes). Then the power spectrum of each component is calculated for the time period 0300–0600 UT. The two vertical lines in each portion of Figure 6 indicate the frequencies of 0.6 mHz and 1.3 mHz. These are the frequencies that have been identified both in the tail and in the ionosphere by *Lyons et al.* [2002] in association with the PBIs and they are drawn here for reference. All three components of the ion velocity have clear peaks at ~0.7 mHz and 1.4 mHz, although the amplitude of the peaks varies from one component to the next. It is interesting to note that V_x has the higher-amplitude peaks and thus the strongest oscillations at the frequency peaks. The V_y has smaller amplitude peaks but still very significant, while the peaks in V_z are even smaller. The peaks in the magnetic field are not at exactly the same frequencies, but the power spectrum of the B_y component is very similar to the spectrum of the velocity. We do see therefore that the repetitive BBFs and PBIs during the period considered here are characterized by oscillations in the tail at the two characteristic frequencies that were reported before by *Lyons et al.* [2002]. We have not analyzed other data for this event with respect to this ULF oscillation as this is not the primary goal of this paper. We are therefore unable to say whether these oscillations observed by Geotail are global in this case or not and whether they are externally driven or not. We have however shown that these frequencies, 0.7 mHz and 1.4 mHz in this case, do exist in the plasma sheet during the period of repetitive BBFs and PBIs and their possible connection should be investigated in more depth in the future.

3.2. Orientation of PBIs in the Aurora

[26] Figure 5 shows that the strongest earthward ion flows during the BBFs also had a significant dawnward component. The average flow is also in that direction before and

after the repetitive BBFs of 0400–0600 UT (not shown here), albeit much smaller in average magnitude. There is thus the indication that the plasma sheet two-dimensional flow during this event is earthward and dawnward, at least on the dawnward side of the midtail where Geotail was located. The possible inference is that the fast flow channels in the tail would also be aligned not with the X_{GSM} but rather in the direction of the maximum flow vectors shown in Figure 5. Such a flow channel when projected in the ionosphere would possibly create PBIs that are aligned along a line that goes through 1700 MLT and 0300 MLT, that is, as PBIs are aligned in Figure 4a. If our conjecture is correct then the large V_y velocities observed along with the large V_x velocities at Geotail could explain the particular orientation of the PBIs in the ionosphere.

[27] The IMF conditions may affect the plasma flow in the tail. IMF B_z was strongly negative (−4 to −6.5 nT) and IMF B_y was strongly positive (5.5 to 9.0 nT) during this period. It is unknown whether the large B_y will affect the orientation of the tail convection, and if so how. There are unfortunately no prior studies that show the two-dimensional convection flow in the plasma sheet under positive or negative IMF B_y. Nevertheless, the IMF B_y (along with the negative IMF B_z) should influence the orientation of the electric field in the tail.

[28] Although we do not have full information of the electric field (only the x and y components are available from the electric field instrument) the observations show clearly a sunward component to the electric field in addition to the dawn-dusk component (data not shown here). This would give flow that is both earthward and dawnward as observed. Thus if the fast flow channels follow the orientation of the background convection, then a flow channel would be oriented earthward and dawnward and would map in the ionosphere to a long narrow structure tilted counterclockwise off the north-south orientation, i.e., in the orientation that we observed the PBIs during our event. We defined that orientation as parallel to a line that goes through the 17 and 03 MLTs.

[29] It should also be noted that *Hori et al.* [2000] and *Kaufmann et al.* [2001] estimated from Geotail data that the electric drift in the tail plasma sheet is in general dawnward on the dawnside and duskward on the duskside, which might in general lead to a dawnward orientation of flow channels on the dawnside if the channels are aligned with the electric drift and not the total drift (which, as shown by *Hori et al.* [2000], is primarily in the x direction on the dawnside).

[30] The suggestions above that the PBI orientation may depend on the IMF B_y need to be investigated on a statistical basis. This is work planned for the future. We would expect the dependence of the PBI orientation on the IMF B_y to be most pronounced during periods of steady and strong B_y and, if such a dependence exists, the orientation of PBIs should be different under negative IMF B_y than it is under positive IMF B_y (because the convection in the plasma sheet is presumably different).

[31] Some encouraging examples from the existing literature include the following events:

[32] 1. 9 February 1997 at ~0330 UT from *Nakamura et al.* [2001a]. The orientation of the observed streamers is opposite to the ones in the present event, that is., tilted clockwise from the NS meridian. IMF B_y was negative for ~1 hour during the relevant time but quite dynamic, oscillating around the 0 value every hour.

[33] 2. 11 December 1998 at ~0230 UT from *Sergeev* [2002]. The orientation of the observed streamers is like that observed in the present event, and the IMF B_y was steadily and strongly positive as in the present event.

[34] 3. 9 November 1998 at 0600–0700 UT from *Henderson et al.* [2001]. This event is also similar to the present event (counterclockwise tilted streamers and positive IMF B_y).

3.3. Projection of PBIs in the Tail

[35] A possible explanation for the orientation of PBIs given in section 3.2 is that the fast flow channels in the tail follow the direction of the background convection and that the IMF B_y may order the direction of that convection. It is nearly impossible to decipher the orientation of the fast flow channels in the tail observationally because of the lack of sufficient multipoint observations. Alternatively, we use the auroral signature to qualitatively determine the orientation of the flow channels by projecting the PBI structures to the tail using the T96 model [*Tsyganenko*, 1996].

[36] Figure 7 shows the PBIs observed by IMAGE FUV for the last eight times shown in Figure 4a. Figure 7 shows (left) the FUV images and (right) the projection of these images to the equatorial plane (region of minimum magnetic field strength **B**). By showing intensities above a threshold in the FUV images of Figure 7, we see only the brightest auroral emissions and individual PBI structures are seen isolated from the background emissions. Some equatorial auroral features were also isolated (e.g., in the 0415:28 UT image around 0000 MLT and in the images of 0437:58 UT and 0440:01 UT after 0300 MLT). These features are not PBIs.

[37] We used the T96 magnetic field model with the IGRF model for near the Earth. The projections of the ionospheric signatures are plotted with the same color scale as the ionospheric signatures (Figure 7, right) and the small red diamond denotes the location of Geotail in the XY plane. For a selection of images we have marked individual features (mostly PBIs) as 1, 2, 3, etc. (Figure 7, left) and then marked the projections of these same features on Figure 7 (right) similarly. This should aid the reader in understanding how each feature is projected in the tail with the T96 model.

[38] There are a few interesting observations that result from this exercise. First of all and most striking is the fact that all the PBIs, both the primarily NS ones near 0000 MLT and the primarily EW ones near 1900 MLT, map out to stretched, narrow channels that are mostly radial and do not have a dawnward orientation as suggested in section 3.2. PBIs in the premidnight region tend to stretch farther downtail than do the postmidnight ones at similar latitudes (see for example the projections on 0502:31 UT and 0506:37 UT). These results are in apparent contradiction with our deductions in section 3.2. It is impossible at this point for us to judge whether the deductions or the mappings are correct. Further future research needs to be done to determine reliably the orientation of the PBI mappings to the equatorial plane and of the flow channels in the plasma sheet.

[39] In some cases a single elongated PBI in the premidnight ionosphere projects to a connected set of almost

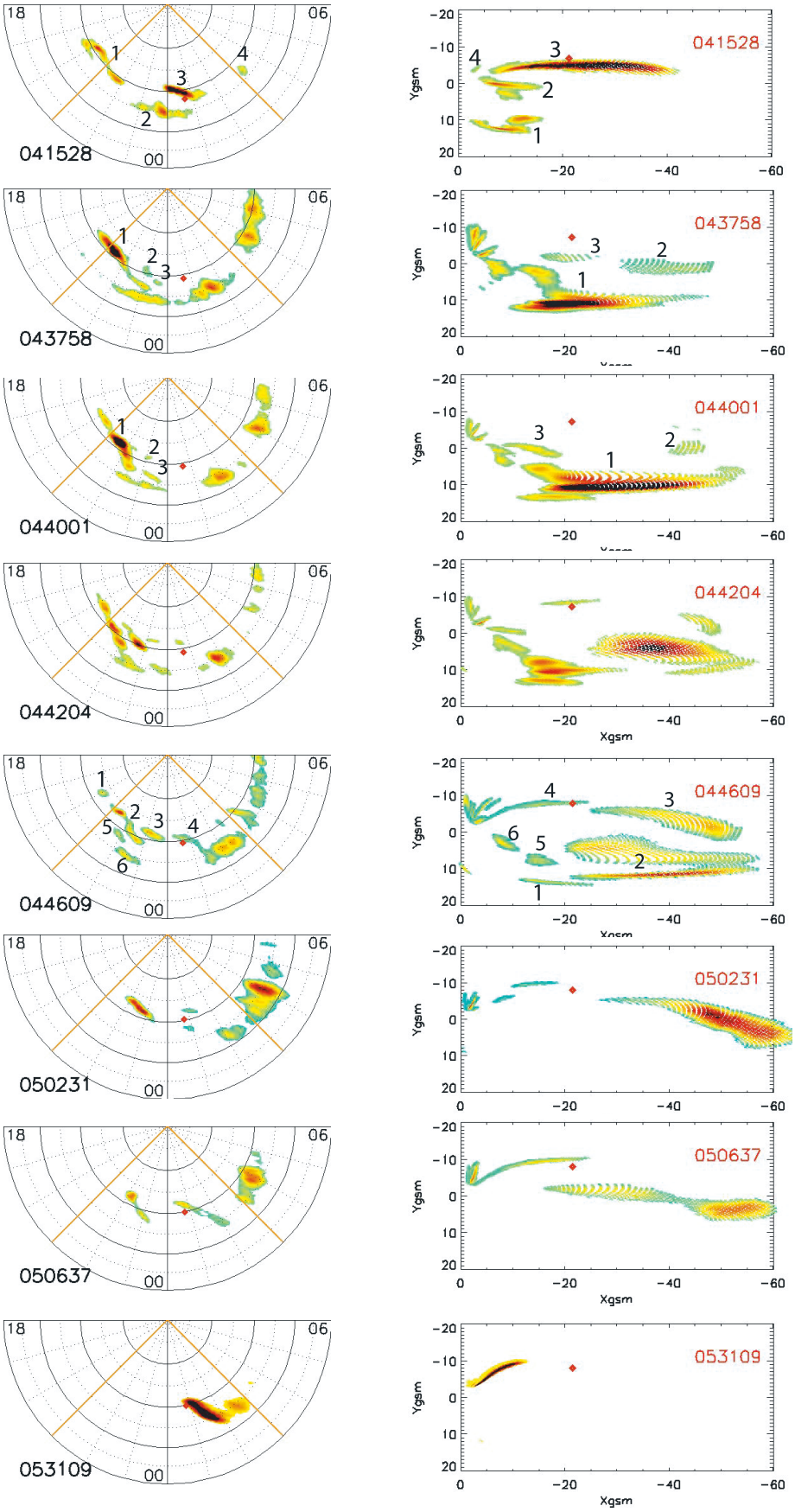

Figure 7. Tail projections of PBIs observed by IMAGE FUV for the last eight times shown in Figure 4a. (left) FUV images; (right) T96 projection of these images to the equatorial plane.

parallel stretched channels in the tail. This is the case for feature 1 in the image of 0440:01 UT and feature 2 in the image of 0446:09 UT. We are not able to ascertain if this geometry is realistic. However, it does not happen for postmidnight PBIs, so again we see that the projections for similar features are very different on the two sides of local midnight.

[40] The projection of 0446:09 UT illustrates the possible dynamical state of the plasma sheet during multiple PBIs. If we associate each PBI with a flow channel, then we infer that multiple, parallel fast flow channels extend across the width of the plasma sheet. This particular image is similar to the cartoon shown by *Sergeev et al.* [2000, their Figure 3], where the existence of multiple such channels had been postulated. *Sergeev et al.* [2000] assumed that intermittent reconnection at a distant X line would be associated with the observed fast flows, consistent with the observations by *de la Beaujardière et al.* [1994] that flow bursts associated with the PBIs extend across the ionospheric mapping of the separatrix. Since such flow channels have been observed to be azimuthally narrow, this leads to the inference that each PBI should be associated with a region of enhanced reconnection that is localized in y along the tail X line. If this is correct, then the projections we show in Figure 7 indicate that each reconnection region is associated with flow enhancements that extend long distances in the x direction, and the origin of these reconnection regions is anywhere from X ~ -30 R_E to X ~ -70 R_E or more at any one instant. However, how such an inference is connected with a single distant X line needs to be understood. *Lyons et al.* [2002] suggested that PBIs and midtail BBFs may be a manifestation of a global ULF mode with frequencies of 0.5–0.7 mHz and its harmonic of 1.1–1.3 mHz. Under this suggestion, it would be the ULF oscillation itself that leads to the strong y dependence of reconnection across the tail. This could be either externally driven by the solar wind, if the ULF pulsations are the result of solar wind dynamic pressure variations as suggested by *Kepko and Spence* [2003], or the result of wave generation either within the magnetosphere or by magnetosheath flows [e.g., *Mann et al.*, 1999].

[41] Finally, we should caution that the projections in Figure 7 should only be considered as tentative and qualitative. The T96 model can give highly unreliable mappings on strongly stretched magnetic field lines. *Sergeev* [2002] discussed problems with mapping of narrow structures from the tail to the ionosphere. The ionosphere-mapped image of the tail source can be significantly rotated because of distortions from field-aligned currents and field-aligned potential drops, and the resulting distortions should be most significant along field lines with small equatorial magnetic field. While Figure 2 shows that the magnetic field measured by Geotail was not small, the analysis of *Sergeev* [2002] indicates the uncertainties with mappings such as shown in Figure 7.

[42] It is very difficult to validate such projections with presently available data. We also found that the projections may vary depending on whether we use the T96 with a dipole field model instead of the IGRF model, since the IGRF model has UT dependence and the dipole does not. A way to test how accurate the T96 projection might be is to compare the model-determined magnetic field at the location of Geotail with the observed magnetic field. The dashed lines in Figures 2a–2d are the T96 model magnetic field components at the location of Geotail for the period 0200–0700 UT. The model values are calculated every 5 minutes. The model field is excellent for the B_y component and it is reasonable for the B_x component, although it cannot reproduce the transfer of the spacecraft from near the lobes to the central current sheet. The model B_z is however much smaller than the observed component and the same holds true for the magnetic field magnitude. Thus we feel that all the points discussed in the present section should be taken as only indications or suggestions.

4. Summary and Conclusions

[43] On 3 January 2001, after the end of the expansion phase of a substorm and during the time period 0320–0520 UT, a series of equatorward extending PBIs were observed by the Rankin Inlet MSP located in the premidnight region. Geotail, located dawnward of the noon-midnight meridian in the midtail plasma sheet, observed a series of repetitive BBFs during approximately the same time period, 0400–0545 UT. The footprint of Geotail remained in the 0100–0230 MLT region. The IMF B_z was strongly southward and the IMF B_y was strongly positive. A one-to-one correlation between PBIs and BBFs cannot be found in these two data sets, unlike what we have found when the MSP and Geotail are near the same longitude [*Zesta et al.*, 2000]. Global auroral observations by the IMAGE FUV imager from the same time period have given us the opportunity to put the other two data sets into perspective and draw significant conclusions for the global occurrence of PBIs and their associated BBFs.

[44] We examined the series of auroral images from the whole nightside from the IMAGE FUV instrument for the period 0200–0600 UT. In each auroral image we identified the field of view of the Rankin Inlet MSP and the ionospheric footprint of the Geotail spacecraft. The Rankin Inlet MSP moved from 2100 MLT to 2300 MLT during the period studied, while the ionospheric footprint of Geotail remained in the 0130–0230 MLT region. So, even though there was never a good local conjunction between the Rankin Inlet MSP and Geotail, the FUV was in continuous conjunction with both the ground MSP and with Geotail. We were thus able to relate PBI signatures seen in the MSP with EW or NS PBIs observed by the FUV inside the field of view of the ground MSP. Simultaneously we were able to relate fast flow signatures, or the lack thereof, observed by Geotail with specific NS PBIs observed by FUV.

[45] We were able to deduce that every single PBI structure must be associated with a fast flow channel in the tail within the same local time sector. Thus PBIs correlate well with plasma sheet fast flows observed only within the local time sector of the PBIs. Furthermore, in the local time sector where PBIs are not seen in the ionosphere no fast flows are seen in the tail. While this result was directly deduced only from the local time sector of Geotail, our results are certainly consistent with a general one-to-one correspondence between BBFs and equatorward extending PBIs. Clearly, a larger number of events need to be thus examined to establish the generality of our single-event conclusion.

[46] Multiple PBIs can occur over the whole width of the nightside aurora or in a more restricted local sector. This directly implies that many fast flow channels exist simultaneously over a width of the plasma sheet at a given time, and this width can cover the whole width of the plasma sheet or only a part of it.

[47] We found that the orientation and structure of PBIs is locally time dependent. Most are narrow structures that are tilted counterclockwise off the north-south direction and are thus aligned with a line that goes approximately through the 0300 and 1700 MLTs. Thus PBIs are seen as NS in the postmidnight sector and as EW arcs closer to the dusk sector. Observations of the local time dependence of the orientation of streamers have been reported before [e.g., *Henderson et al.*, 1994; *Sergeev*, 2002]. *Henderson et al.* [1994], for example, also found that streamers are more east-west aligned closer to dusk and more north-south near midnight. Most PBIs observed with IMAGE during this event in the premidnight sector are EW arcs that initiate near the poleward boundary and then propagate equatorward. They often tilt and become ~NS structures as they propagate equatorward and duskward. This suggests that the same dynamics (i.e., fast flow channels) may produce both EW and NS PBI structures.

[48] In examining the reason for that particular orientation of PBIs, we suggested that large V_y velocities that exist in the tail during the PBI fast flows may be the result of the tail convection being earthward and dawnward during positive IMF B_y. This offers a possible reason for the alignment of PBIs in the ionosphere along the 0300–1700 MLT line and why PBIs start as EW and turn to NS structures. However, the projection of the PBI structures into the tail using the T96 model suggests that all PBIs, both EW and NS, map to radially stretched channels in the tail with no dawnward component. This issue needs to be resolved in the future as neither the suggestion of the IMF B_y ordering the tail convection or the T96 mappings has been verified.

[49] Finally, frequency analysis indicates that the PBI/BBF period is characterized by oscillations in the velocity and magnetic field with frequencies of ~0.6 mHz and ~1.3–1.5 mHz. This oscillation in velocity is superposed in the background strong convection. We briefly reviewed two suggestions for the source of PBIs and BBFs, intermittent distant X line reconnection [*Sergeev et al.*, 2000] and a global ULF pulsation [*Lyons et al.*, 2002], and suggested that these two processes may be related.

[50] **Acknowledgments.** This research was supported at UCLA by NSF grants OPP-0136139 and ATM-0207298. Support for the operations of the CANOPUS MSP is provided by the Canadian Space Agency. We thank J. C. Samson, who provided us with the algorithm for merging the Gillam and Rankin Inlet photometer data and with access to the MSP data. DMSP image and data processing is by NOAA's National Geophysical Data Center. DMSP data was collected by the U.S. Air Force Weather Agency.

[51] Arthur Richmond thanks Victor Sergeev and Michael G. Henderson for their assistance in evaluating this paper.

References

Allan, W., and A. N. Wright (2000), Magnetotail waveguides: Fast and Alfvén waves in the plasma sheet boundary layer and lobes, *J. Geophys. Res.*, *105*, 317.

Angelopoulos, V., W. Baumjohann, C. F. Kennel, F. V. Coroniti, M. G. Kivelson, R. Pellat, R. J. Walker, H. Lühr, and G. Paschmann (1992), Bursty bulk flows in the central plasma sheet, *J. Geophys. Res.*, *97*, 4027.

Angelopoulos, V., et al. (1994), Statistical characteristics of bursty bulk flow events, *J. Geophys. Res.*, *99*, 21,257.

Baumjohann, W., G. Paschmann, N. Sckopke, C. A. Cattell, and C. W. Carlson (1988), Average ion moments in the plasma sheet boundary layer, *J. Geophys. Res.*, *93*, 11,507.

Baumjohann, W. J., G. Paschmann, and H. Lühr (1990), Characteristics of high-speed flows in the plasma sheet, *J. Geophys. Res.*, *95*, 3801.

Blanchard, G. T., L. R. Lyons, and J. C. Samson (1997), Accuracy of 6300 Å auroral emission to identify the separatrix on the nightside of the Earth, *J. Geophys. Res.*, *102*, 9697.

Chen, C. X., and R. A. Wolf (1993), Interpretation of high-speed flows in the plasma sheet, *J. Geophys. Res.*, *98*, 21,409.

de la Beaujardière, O., et al. (1994), Quiet-time intensifications along the poleward auroral boundary near midnight, *J. Geophys. Res.*, *99*, 287.

Eastman, T. E., L. A. Frank, W. K. Peterson, and W. Lennartsson (1984), The plasma sheet boundary layer, *J. Geophys. Res.*, *89*, 1553–1572.

Eastman, T. E., L. A. Frank, and C. Y. Huang (1985), The boundary layers as the primary transport regions of the Earth's magnetotail, *J. Geophys. Res.*, *90*, 9541–9560.

Henderson, M. G., J. S. Murphree, and G. D. Reeves (1994), The activation of the dusk-side and the formation of north-south aligned structures during substorms, in *Substorms 2: Proceedings of the Second International Conference on Substorms, March 7–11, 1994, University of Alaska at Fairbanks, Fairbanks, Alaska*, edited by J. R. Kan, J. D. Craven, and S.-I. Akasofu, p. 37, Geophysical Institute, Univ. of Alaska Fairbanks, Fairbanks, Alaska.

Henderson, M. G., G. D. Reeves, and J. S. Murphree (1998), Are north-south structures an ionospheric manifestation of bursty bulk flows?, *Geophys. Res. Lett.*, *25*, 3737.

Henderson, M. G., L. Kepko, H. E. Spence, M. Connors, J. B. Sigwarth, L. A. Frank, H. J. Singer, and K. Yumoto (2001), The evolution of north-south aligned auroral forms into auroral torch structures: The generation of omega bands and Ps6 pulsations via flow bursts, *Eos Trans. AGU*, *82*(47), Fall Meet. Suppl., Abstract SM51B-0809.

Hori, T., K. Maezawa, Y. Saito, and T. Mukai (2000), Average profile of ion flow and convection electric field in the near-Earth plasma sheet, *Geophys. Res. Lett.*, *27*, 1623.

Kaufmann, R. L., B. M. Ball, W. R. Paterson, and L. A. Frank (2001), Plasma sheet thickness and electric currents, *J. Geophys. Res.*, *106*(A4), 6179–6194.

Kauristie, K., V. A. Sergeev, M. Kubyshkina, T. I. Pulkkinen, V. Angelopoulos, T. Phan, R. P. Lin, and J. A. Slavin (2000), Ionospheric current signatures of transient plasma sheet flows, *J. Geophys. Res.*, *105*, 10,677.

Kauristie, K., V. A. Sergeev, O. Amm, M. V. Kubyshkina, J. Jussila, E. Donovan, and K. Liou (2003), Bursty bulk flow intrusion to the inner plasma sheet as inferred from auroral observations, *J. Geophys. Res.*, *108*(A1), 1040, doi:10.1029/2002JA009371.

Kepko, L., and H. E. Spence (2003), Observations of discrete, global magnetospheric oscillations directly driven by solar wind density variations, *J. Geophys. Res.*, *108*(A6), 1257, doi:10.1029/2002JA009676.

Kokubun, S., T. Yamamoto, M. H. Acuna, K. Hayashi, K. Shiokawa, and H. Kawano (1994), The geotail magnetic field experiment, *J. Geomagn. Geoelectr.*, *46*, 7–21.

Lyons, L. R., T. Nagai, G. T. Blanchard, J. C. Samson, T. Yamamoto, T. Mukai, A. Nishida, and S. Kokubun (1999), Association between GEOTAIL plasma flows and auroral poleward boundary intensifications observed by CANOPUS photometers, *J. Geophys. Res.*, *104*, 4485.

Lyons, L. R., E. Zesta, Y. Xu, E. R. Sánchez, J. C. Samson, G. D. Reeves, J. M. Ruohoniemi, and J. B. Sigwarth (2002), Auroral poleward boundary intensifications and tail bursty flows: A manifestation of a large-scale ULF oscillation?, *J. Geophys. Res.*, *107*(A11), 1352, doi:10.1029/2001JA000242.

Mann, I. R., A. N. Wright, K. J. Mills, and V. M. Nakriakov (1999), Excitation of magnetospheric waveguide modes by magnetosheath flows, *J. Geophys. Res.*, *104*, 333.

McComas, D. J., S. J. Bame, P. Barker, W. C. Feldman, J. L. Phillips, P. Riley, and J. W. Griffee (1998), Solar Wind Electron Proton Alpha Monitor (SWEPAM) for the Advanced Composition Explorer, *Space Sci. Rev.*, *86*, 563–612.

Mende, S. B., et al. (2000), Far ultraviolet imaging from the IMAGE spacecraft: 1. System design, *Space Sci. Rev.*, *91*, 243.

Mukai, T., S. Machida, Y. Saito, M. Hirahara, T. Terasawa, N. Kaya, T. Obara, M. Ejiri, and A. Nishida (1994), The low energy particle (LEP) experiment onboard the Geotail satellite, *J. Geomagn. Geoelectr.*, *46*, 669–692.

Nakamura, R., W. Baumjohann, M. Brittnacher, V. A. Sergeev, M. Kubyshkina, T. Mukai, and K. Liou (2001a), Flow bursts and auroral activations: Onset timing and foot point location, *J. Geophys. Res.*, *106*, 10,777.

Nakamura, R., W. Baumjohann, R. Schödel, M. Brittnacher, V. A. Sergeev, M. Kubyshkina, T. Mukai, and K. Liou (2001b), Earthward flow bursts, auroral streamers, and small expansions, *J. Geophys. Res.*, *106*, 10,791.

Samson, J. C., and R. Rankin (1994), The coupling of solar wind energy to MHD cavity modes, waveguide modes, and field line resonances in the Earth's magnetosphere, in *Solar Wind Sources of Magnetospheric ULF Pulsations*, edited by M. J. Engebretson, K. Takahashi, and M. Scholer, p. 253, AGU, Washington, D. C.

Sergeev, V. A. (2002), Ionospheric signatures of magnetospheric particle acceleration in substorms—How to decode them?, in *Proceedings of the 6th International Conference on Substorms*, pp. 39–46, Univ. of Washington, Seattle, Wash.

Sergeev, V. A., K. Liou, C.-I. Meng, P. T. Newell, M. Brittnacher, G. Parks, and G. D. Reeves (1999), Development of auroral streamers in association with impulsive injections to the inner magnetotail, *Geophys. Res. Lett.*, *26*, 417.

Sergeev, V. A., et al. (2000), Multiple-spacecraft observation of a narrow transient plasma jet in the Earth's plasma sheet, *Geophys. Res. Lett.*, *27*, 851.

Smith, C. W., J. L'Heureux, N. F. Ness, M. H. Acuna, L. F. Burlaga, and J. Scheifele (1998), The ACE Magnetic Fields Experiment, *Space Sci. Rev.*, *86*, 613–632.

Tsyganenko, N. A. (1996), Effects of the solar wind conditions on the global magnetospheric configuration as deduced from data-based field models, *Eur. Space Agency Spec. Publ.*, *ESA SP 389*, 181.

Zesta, E., L. R. Lyons, and E. Donovan (2000), The auroral signature of Earthward flow burst observed in the magnetotail, *Geophys. Res. Lett.*, *27*, 3241–3244.

Zesta, E., E. Donovan, L. Lyons, G. Enno, J. S. Murphree, and L. Cogger (2002), The two-dimensional structure of auroral poleward boundary intensifications (PBIs), *J. Geophys. Res.*, *107*(A11), 1350, doi:10.1029/2001JA000260.

E. Donovan, Physics Department, University of Calgary, 2500 University Drive NW, Calgary, Alberta T2N 1N4, Canada.

H. Frey, Space Sciences Laboratory, University of California, Berkeley, Grizzly Peak at Centennial Dr., Berkeley, CA 94720-7450, USA.

L. Lyons, C.-P. Wang, and E. Zesta, Department of Atmospheric and Oceanic Sciences MS-71, University of California, Los Angeles, Box 951565, 405 Hilgard Avenue, Los Angeles, CA 90095-1565, USA. (ezesta@atmos.ucla.edu)

T. Nagai, Department of Earth and Planetary Sciences, Tokyo Institute of Technology, Ookayama 2-12-1 Meguro, Tokyo 152-8551, Japan.